CSIRO PUBLISHING
www.publish.csiro.au/journals/fpb *Functional Plant Biology*, 2003, **30**, 785–796

Characterization of the 820-nm transmission signal paralleling the chlorophyll *a* fluorescence rise (OJIP) in pea leaves

Gert Schansker[A,D], *Alaka Srivastava*[B], *Govindjee*[C] *and Reto J. Strasser*[A]

[A]Bioenergetics Laboratory, Geneva University, CH-1254 Jussy, Geneva, Switzerland.
[B]Biochemistry and Biophysics, University of Rochester Medical Center, Rochester, NY, 14642, USA.
[C]Department of Plant Biology, 265 Morill Hall, University of Illinois, Urbana, IL, 61801–3707, USA.
[D]Corresponding author; email: Gert.Schansker@bioen.unige.ch

Abstract. Monitoring transmission changes at 820 nm, a measure of the redox states of plastocyanin (PC) and P700, is a good complementary technique for chlorophyll (chl) *a* fluorescence induction measurements. A thorough characterization of the properties of the 820-nm transmission kinetics during the first second after a dark-to-light transition is provided here for pea (*Pisum sativum* L.) leaves. The data indicate that plastocyanin in a dark-adapted leaf is in the reduced state. Three photosystem I (PSI)-related components, PC, P700 and ferredoxin, can contribute to the 820-nm transmission signal. The contribution of ferredoxin, however, is only approximately 5%, thus, it can be neglected for further analysis. Here, we show that by monitoring the sequential oxidation of PC and P700 during a far-red pulse and analysing the re-reduction kinetics it is possible to assign the three re-reduction components to PC (τ = 7–14 s) and P700 (τ = 35–55 ms and 1.2–1.6 s). Our data indicate that the faster re-reduction phase (τ = 35–55 ms) may represent a recombination reaction between $P700^+$ and the acceptor side of PSI. This information made it possible to show that the ratio between the potential contributions of PC : P700 is 50 : 50 in pea and *Camellia* leaves and 40 : 60 in sugar beet leaves.

Keywords: chlorophyll fluorescence, DCMU, pea, plastocyanin, plastoquinone pool, P700, re-reduction kinetics, stromal electrons, 820-nm transmission.

Introduction

The photosynthetic electron transport chain consists of three large protein complexes — photosystem II (PSII), cytochrome (cyt) b_6/f and photosystem I (PSI) connected by two mobile electron carriers, plastoquinone (PQ) and plastocyanin (PC) (see Ke 2001). In a dark-adapted leaf the electron transport chain is mainly in the oxidized state.

Induction of photosynthesis leads, initially, to an almost complete reduction of the electron transport chain (ETC) followed by an activation of the enzyme ferredoxin–$NADP^+$ reductase (FNR) and the Calvin–Benson cycle, and a subsequent partial re-oxidation of the reduced ETC (Foyer *et al.* 1992). This initial reduction process is represented by the O–J–I–P steps of the Kautsky curve during chlorophyll (chl) *a* fluorescence measurements. The plastoquinone pool, plastocyanin and PSI are involved in the J–I–P part of the chl *a* fluorescence induction curve, but the interpretation of these steps is presently being contested (see Samson *et al.* 1999 for a review).

Oxidation of the reaction center chls of PSI, P700, is known to cause an increase in absorbance in the 800–850 nm range, in addition to an absorbance decrease at 700 nm (see chapters 28 and 30 in Ke 2001). Monitoring absorbance and/or transmission changes near 820 nm is a very convenient way to follow the redox state of P700 under continuous light (Harbinson and Woodward 1987; Schreiber *et al.* 1988; Harbinson and Hedley 1989; Klughammer and Schreiber 1994). Light of 820 nm is not actinic and thus, it is possible to utilize high light intensities without disturbing the system. Measuring chl *a* fluorescence and transmission at 820 nm simultaneously makes it possible to study electron transfer processes during induction at the two ends of the electron transport chain.

Abbreviations used: chl, chlorophyll; cyt, cytochrome; DCMU 3-(3,4-dichlorophenyl)-1,1′-dimethylurea; ETC, electron transport chain; FNR, ferredoxin–$NADP^+$ reductase; *I*, photocurrent, a measure for the transmitted light; I_t, photocurrent at time *t*; LED, light-emitting diode; OJIP curve, fluorescence induction curve defined by the names of its intermediate steps, O-level equals F_o and is initial, minimal, fluorescence, J-level equals fluorescence level at ~2 ms, I-level equals fluorescence level at ~20 ms and P-level equals F_m, the maximum fluorescence; PAR, photosynthetically active radiation; PC, plastocyanin; P680 and P700, reaction center pigments of photosystem II and I, respectively; Q_A, primary quinone electron acceptor of photosystem II; τ, time for a reaction to reach 63% completion (1/e of original state remaining).

 10.1071/FP03032 1445-4408/03/070785

A problem is that, in practice, three components contribute to the absorbance and/or transmission changes in the 820 nm range, PC, P700 and ferredoxin (Klughammer and Schreiber 1991). Harbinson and Hedley (1989) estimated, on the basis of spectra from Ke (1973) and Katoh (1977), that PC contributed approximately 35% of the total absorbance change at 820 nm. Klughammer and Schreiber (1991), using chloroplast suspensions, attempted to determine the potential contribution of several components to the absorbance changes at 820 nm, namely P680, P700, PC, ferredoxin, and an electrochromic change. They calculated a potential contribution of PC to the absorbance changes at 830 nm of 37%. For steady-state measurements it has been assumed that the redox states of PC and P700 change in parallel (Harbinson and Hedley 1993). However, during photosynthetic induction an electron transfer balance between PSII and PSI still has to be established, and strong swings in the redox states of the components around PSI occur (Laisk *et al.* 1992*a*). No parallelism in the behavior of PC and P700 is expected here.

To date, most of the attention has been focused on the determination of the P700 re-reduction kinetics in darkness (Harbinson and Hedley 1989; Ott *et al.* 1999; Clarke and Johnson 2001, Eichelmann *et al.* 2000) and on measurements of the quantum yield of PSI, to determine whether PSII and PSI are strictly coupled to CO_2 fixation or whether electrons are lost in alternative pathways (Harbinson *et al.* 1989; Weis and Lechtenberg 1989; Klughammer and Schreiber 1994). Harbinson and Hedley (1993) studied the kinetics of the 820-nm signal during the first 100 s after a dark–light transition, but their analysis started approximately 1 s after lights were turned on. Much of the early information was, therefore, missing. Thus, it was necessary to characterize the properties of the 820-nm transmission signal during the first second in order to be able to use it as a complementary technique for chl *a* fluorescence induction measurements.

The goal of this study was to understand changes in the 820-nm transmission during approximately the first second after a dark-to-light transition, in order to be able to use this technique to complement chl *a* fluorescence induction (OJIP) measurements. The second goal of the study was to find a way to separate, by kinetic means, the contributions of plastocyanin and P700 to the transmission at 820 nm.

Materials and methods

Plant material

Measurements were made using mature pea leaves (*Pisum sativum* L. cv. Ambassador) (2–3-week-old plants). Plants were grown under long-day conditions in a greenhouse where temperatures were kept at 20–25°C during the day and 14°C during the night. Leaves of a pot-grown *Camellia* plant (*Camellia japonica* L.) and leaves of hydroponically-grown sugar beet plants (*Beta vulgaris* L.) were also used, under the same temperature regime as the pea plants.

Measuring equipment

The measurements were made using a PEA (Plant Efficiency Analyser) senior (Hansatech Instruments, Kings Lynn, Norfolk, UK). This instrument allows the simultaneous measurement of the chl *a* fluorescence transient (OJIP curve) and of the 820-nm transmission change. The first reliable measuring point for fluorescence change was at 20 μs, whereas the first measuring point for transmission change was at 400 μs. The time constant used for the transmission measurements was 100 μs. The light intensity used for all experiments was 1800 μmol photons m^{-2} s^{-1}. The light was produced by four 650-nm LEDs (light-emitting diodes). The far-red source was a QDDH73520 LED (Quantum Devices Inc., Barneveld, WI, USA) filtered 720 ± 5 nm. The modulated (33.3 kHz) far-red measuring light was provided by an OD820 LED (Opto Diode Corp., Newbury Park, CA, USA) filtered 830 ± 20 nm. Executing commands such as turning on and off the LEDs took approximately 250 μs. Turning on the red light and starting the measurement were synchronized commands. For the far-red light there was a delay of 250 μs between turning on the far-red light and the start of the measurement. Each measurement consisted of three parts. First, the transmission was measured without amplification, and offset to obtain a value for total transmission (I_0). Subsequently, the transmission was measured with a gain of 50 to obtain a value for the transmission at $t = 0$. This was followed by kinetic measurements.

From the light intensity dependence of the J-level of chl *a* fluorescence transients, we estimated that for our pea leaves 1800 μmol photons m^{-2} s^{-1} was equivalent to approximately one photon absorbed per reaction center antenna per 320 μs (not shown). According to Harbinson and Hedley (1993), 2000 μmol photons m^{-2} s^{-1} photosynthetically active radiation (PAR) equals approximately one P700 excitation per ms for pea leaves.

The experiments shown in Fig. 1 show that the equipment can achieve full oxidation of PC and P700, and demonstrate, at the same time, how the maximum reducible/oxidizable amplitude was determined. In Fig. 1*A* the electron transport chain was reduced by a 1-s red light pulse of 1800 μmol photons m^{-2} s^{-1} [phase 1; see Fig. 1*B* where the same curve is plotted on a log scale with better time resolution (■)], subsequently oxidized by a 10-s far-red pulse of 200 μmol photons m^{-2} s^{-1} [phase 2; see also (●) in Fig. 1*B*] and finally, reduced again by a 2-s red light pulse (phase 3). The red LEDs (reaching their maximum intensity on a sub microsecond time scale) will, initially, oxidize all P700 that was left un-oxidized by the far-red pulse [see first few ms, phase 3 in Fig. 1*B* (▲)] and, subsequently, reduce the whole electron transport chain. The added advantage of the red-light pulse is that it is short enough to avoid any contribution of drift of the base line. The difference between the minimum and the maximum of phase 3 was used to define the maximum reducible/oxidizable amplitude (= transmission difference between all PC, P700 and ferredoxin oxidized and reduced, respectively). Comparing the two traces shown for phase 2 (closed symbols indicate with and open symbols indicate without red pulse) it becomes clear that the final transmission level reached by the far-red pulse is independent of the redox state of the electron transport chain and thus, that a limitation on the acceptor side of PSI doesn't play a role under our experimental conditions.

DCMU treatment

For the measurements made in the presence of DCMU [3-(3,4-dichlorophenyl)-1,1′-dimethylurea], leaves were submerged in a solution of 100 μM DCMU containing 1% ethanol (v/v) for 15, 30 or 60 min in darkness. The leaves were subsequently dried with tissue and kept in complete darkness for 30 min, followed by another 30 min in the leaf clip before the measurement was made. By this method the F_o level was hardly affected by the DCMU treatment and the F_m level of chl *a* fluorescence of DCMU-treated leaves was very close to that of a

control leaf. When the leaves were treated with a 1% ethanol solution no effect on the induction curves was observed. To obtain an estimate for the DCMU-induced inhibition of PSII, the following formula was used: per cent inhibition = $(P_{inhibited} - J_{inhibited})/(P_{control} - J_{control}) \times 100$. For an estimation of the inhibition of whole-chain electron transport, we made use of the extent of reversal of the transmission after 100 ms: per cent inhibition = [$I_{100\ ms}$ (fully inhibited) − $I_{100\ ms}$ (intermediate inhibition)]/[$I_{100\ ms}$ (fully active) − $I_{100\ ms}$ (fully inhibited)] × 100.

Presentation of the experimental results

To ensure the transmission measurement remains in the measuring window, the transmission is set to a preset value at the beginning of the second part of the measurement protocol (see Measuring equipment). In the various figures, the transmission is expressed either as a fraction of the total transmission or a bar indicating a measure of this fraction is added to the figure and in that case, the transmission changes are expressed in mV. The enzyme FNR is known to be inactive in a dark-adapted leaf (Carrillo and Vallejos 1987), initially preventing a fast re-oxidation of the acceptor side of PSI and, as a consequence, after 200–300 ms the electron transport chain becomes totally reduced. This is the best reference transmission value, and where possible the data were equalized to this level.

Results

Induction kinetics of chlorophyll a *fluorescence and 820-nm transmission*

Figure 2 shows the simultaneously-measured chl *a* fluorescence and transmission-change kinetics at 820 nm during the first second of illumination with 1800 μmol photons m^{-2} s^{-1} of 650-nm light after a dark adaptation of approximately 5 min. Figure 2*A* shows the traces on a logarithmic time scale and Fig. 2*B* on a linear time scale. In the inset of Fig. 2*A*, the first 8 ms of the transmission change data are plotted on a linear time scale to show that the transmission at 820 nm starts to decrease immediately after the onset of the light. Comparing Fig. 2*A* and its inset, it is worth noting that an exponential function plotted on a logarithmic time scale becomes sigmoidal. Figure 2*A* shows that after about 20 ms the decrease in transmission is replaced by an increase in transmission. At the same time, the I-level is reached in the fluorescence induction curve. We note that 20 ms is also the halftime for the re-oxidation of a plastoquinone molecule by cyt b_6/f (e.g. Witt 1971; Van Voorthuysen 1997; Kramer *et al.* 1999).

DCMU

To test if the reversal of the transmission decrease observed at 20 ms in Fig. 2 was induced by the arrival of electrons from PSII, a series of measurements were made in the presence of DCMU, which inhibits electron flow from PSII to cyt b_6/f. Figure 3 shows the effects of DCMU on both the fluorescence induction (Fig. 3*A*) and the transmission at 820 nm (Fig. 3*B*). When electron flow out of PSII is completely blocked (60 min incubation with 100 μM DCMU; trace d, Fig. 3*B*), the transmission decrease, instead of reversing after 20 ms, decreased further beyond this point. At the same time, chl *a* fluorescence reached its maximum value (all Q_A being in reduced state, trace d, Fig. 3*A*). In Fig. 3 two other traces (b and c) indicate that DCMU only partially blocked electron flow from PSII to PSI. The traces b show that 35% inhibition of PSII (Fig. 3*A*) had no effect on electron transfer through PSI (Fig. 3*B*) and the traces c show that for a 70% block of whole-chain electron transfer (Fig. 3*B*), approximately 95%

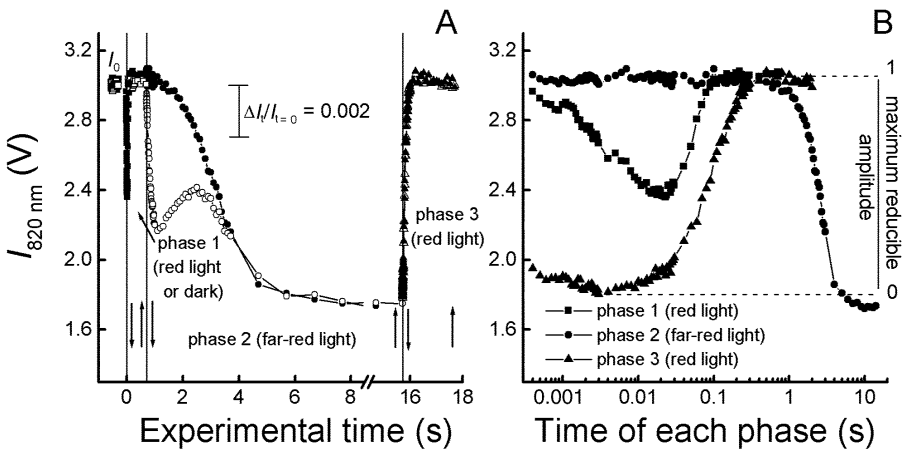

Fig. 1. Protocol to determine the maximum reducible/oxidizable amplitude at 820 nm for a pea leaf. Transmission at 820 nm is plotted against time. (*A*) The three phases of the protocol are presented (filled symbols): phase 1, 0.7 s, 1800 μmol m^{-2} s^{-1} red light; phase 2, 15 s, 200 μmol m^{-2} s^{-1} far-red light; phase 3, 2 s, 1800 μmol m^{-2} s^{-1} red light. A second set of curves (open symbols) without the first 0.7 s red illumination is also shown. Downward arrows indicate light on and upward arrows indicate light off. The transmission level before illumination (I_0) is indicated before the protocol began. (*B*) the traces in part *A* (for the filled symbols) are overlaid and presented on a logarithmic time scale. The maximum reducible/oxidizable amplitude is derived from the difference between the minimum and maximum transmission level induced by the illumination in phase 3.

of all PSII (Fig. 3*A*) was blocked. This confirms and extends the earlier observations and conclusions of Heber *et al.* (1988) with intact chloroplasts.

Limitation on the acceptor side of PSI

We tested whether the reversal of the transmission decrease at 820 nm, beyond 20 ms, was due to a limitation at the acceptor side of PSI (Figs 4, 5). A transient limitation on the acceptor side has been implied by several authors (Munday and Govindjee 1969; Schreiber *et al.* 1988; Harbinson and Foyer 1991; Foyer *et al.* 1992; Laisk *et al.* 1992*b*). This limitation can either be due to inactive FNR (Carillo *et al.* 1980, 1981; Satoh 1981) or to inactivity of the Calvin–Benson cycle. Harbinson and Hedley (1993) demonstrated that a limitation exists on the acceptor side of PSI for the transmission changes beyond the P-level of chl *a* transient. It is known that at high light intensities $P700^+$ accumulates (Weis and Lechtenberg 1989; Laisk *et al.* 1992*b*) indicating that under these conditions, when the Calvin–Benson cycle is active, electron donation to PSI is limiting. The dark-adaptation kinetics of the 820-nm transmission transient were studied by giving a second 1-s pulse of red (650 nm) light at various times after the first pulse (Fig. 4*A*). A second pulse given at short intervals (0.1 s) after the first 1-s pulse induced only relatively minor changes in the 820-nm transmission transient. At longer intervals (1–2 s) after a 1-s pulse many of the transmission changes found in dark-adapted leaves were observed again. The dark-adaptation kinetics of the transmission transient plotted in Fig. 4*B* show that the signal recovered with a lifetime of ~0.4 s. Data from three different experimental data sets, obtained with two different set-ups (two HandyPEAs for the first set and the integrated PEA senior for the last two measurements) are plotted. Further, the first data set was obtained using separate leaves for each measurement and for the last two data sets a single leaf was used for each series of measurements. Figure 4*B* indicates that the lifetime of recovery of the 820-nm transmission transient (~0.4 s) was independent of the experimental conditions used here.

Effect of Calvin–Benson cycle induction

If the reversal of the transmission decrease at the time between the I- and P-levels of chl *a* fluorescence is caused by a limitation on the acceptor side of PSI, induction of the Calvin–Benson cycle should remove this limitation. In the data shown in Fig. 5, the Calvin–Benson cycle was activated by a 60-s pre-illumination with either 370 (trace b) or 740 (trace c) μmol photons m^{-2} s^{-1} of 650 nm light. Then, after a 'dark-adaptation' of 5 s, a 1-s pulse of 1800 μmol photons m^{-2} s^{-1} was given to probe the transmission transient at 820 nm. The chl *a* fluorescence and 820-nm transmission changes during the 60-s pre-illumination are shown in Figs 5*A* and *B*, respectively. The transmission traces are very comparable to induction kinetics observed by

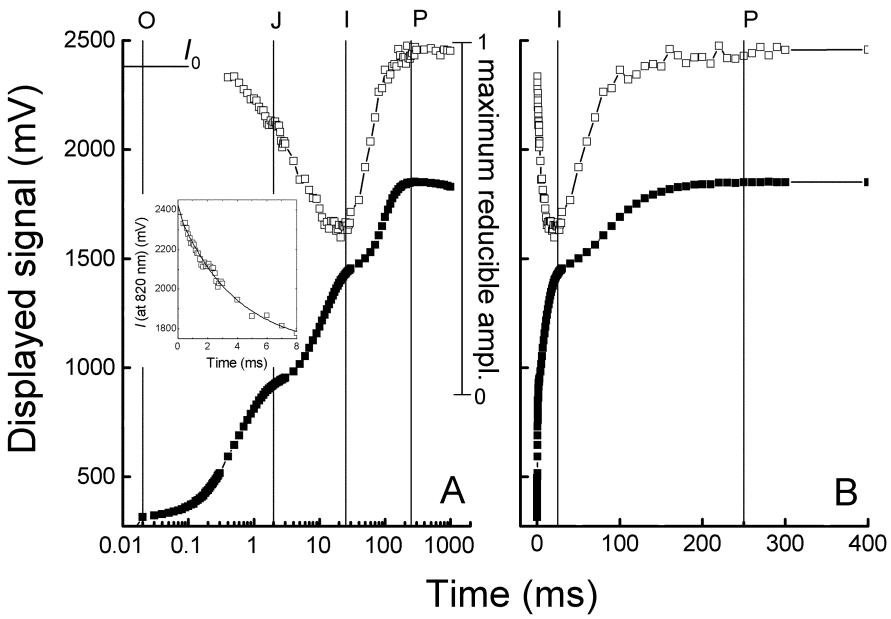

Fig. 2. Simultaneously-measured induction curves of chlorophyll *a* fluorescence (bottom curves) and the transmission at 820 nm (top curves) during the first 2 s after a light–dark transition in pea leaves. (*A*) Signals plotted on a logarithmic time scale; (*B*) the first 400 ms plotted on a linear time scale. The fluorescence levels O, J, I and P are indicated in the figure (see Strasser *et al.* 1995 for the nomenclature used here). The level I_0 indicates the transmission level just before the measurement. The inset of (*A*) shows on a linear time scale the first 8 ms of the transmission changes. The gain of the transmission signal was 50.

Harbinson and Hedley (1993). The accumulation of oxidized P700/PC between 20 and 60 s indicates that the Calvin–Benson cycle was, in fact, induced by the pre-illumination. The experiment demonstrates that a pre-illumination indeed strongly limits the reversal of the transmission changes (compare traces b and c with trace a of Fig. 5*D*). Comparing Figs 5*A* and *B*, it can be noted that 820-nm transmission decrease lagged behind the chl *a* fluorescence decrease in the 10–60 s time range. In Fig. 5*C* the simultaneously-measured chl *a* fluorescence induction curves are plotted for comparison, showing that the effect on transmission is indeed between the I- and P-levels. The pre-illumination caused a strong induction of non-photochemical quenching (decrease of F_m) and the transients behaved as the second pulse of a two-pulse experiment where the maximum fluorescence level is reached after 2 ms (*cf.* Strasser *et al.* 2001), indicating that the plastoquinone pool is still fully reduced. The experiments shown in Figs 4 and 5 indicate that as long as FNR and the Calvin–Benson cycle are inactive, an acceptor-side limitation for PSI exists.

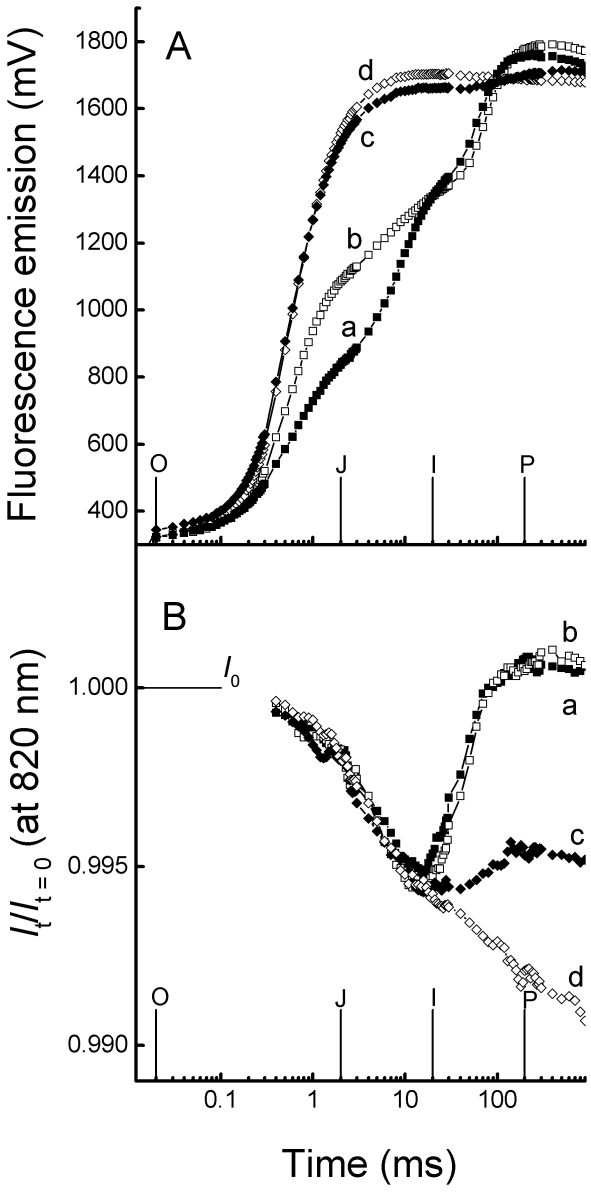

Fig. 3. Effect of DCMU [3-(3,4-dichlorophenyl)-1,1′-dimethyl urea] on the simultaneously-measured induction curves of chlorophyll *a* fluorescence (*A*) and the transmission at 820 nm (*B*). Pea leaves were treated by submerging them for 0 (a), 15 (b), 30 (c) or 60 (d) min in a solution of 100 μM DCMU which contained also 1% ethanol. The leaves were dark-adapted for 60 min before the measurements were made. The level I_0 indicates the transmission level just before the measurement.

External electrons

In the experiments shown in Fig. 6 the electron transport chain was re-oxidized four times by four 15-s pulses of 200 μmol photons m^{-2} s^{-1} far-red (720 nm) light spaced at 100-s intervals. As the far-red light of the first pulse oxidized the system, there was a transient increase in transmission level after about 0.4 s of illumination; this increase peaked at approximately 1 s (Fig. 6*A*). Further pulses (2–4) at 100-s intervals gave smaller increases, indicating that the pool of electrons involved has a limited capacity. After turning off the far-red light, the oxidized components of the electron transport chain will become re-reduced over time and the re-reduction rate depends on the availability of electrons (e.g. Cornic *et al.* 2000). In the experiment shown in Fig. 6*B*, the far-red light was turned off just before, during and after this transient increase of the transmission level, and the subsequent re-reduction kinetics were followed. The traces show that during the transmission increase the re-reduction kinetics were much faster than either before or after the phenomenon. This indicates that the number of electrons available for re-reduction increased. Here, PSII can be excluded as an electron source because the phenomenon disappears on repetition 2–4 of the experiment (Fig. 6*A*). A dark adaptation of 10 min, however, was sufficient to reproduce the trace of the first far-red pulse. This suggests that there is a pool of electrons with a limited capacity that can be donated to the electron transport chain, which needs several minutes to become re-reduced.

Kinetic separation of P700 and PC

Plastocyanin is a fast donor of electrons to oxidized P700, showing halftimes of 10–20 μs for bound PC and 200 μs for free PC (Haehnel *et al.* 1980). This means that during oxidation with far-red light most of the P700 will remain reduced until all PC is oxidized. Assuming that the re-reduction kinetics of both components will be different, it should be possible to separate these components. With this in mind, the experiment shown in Fig. 7 was designed. To minimize interference from the electron pool observed in Fig. 6, the leaves were pre-illuminated for 10 s with 200 μmol photons m^{-2} s^{-1} far-red (720 nm) light, 100 s

before the start of the actual measurement. The inset of Fig. 7*A* illustrates how the experiment works. During oxidation of the electron transport chain the 820-nm transmission level decreased. At the times indicated the far-red light was turned off and the transmission level started to increase again in darkness. Traces are shown for the transmission increase after turning off the far-red light at the time points indicated (Fig. 7*A*). Three exponential functions were fitted to these traces . In Fig. 7*B* the amplitudes of the three fitted components were plotted as a function of the far-red pulse duration. The data in Fig. 7*B* show that the amplitude of the slow phase (lifetime τ = 7–14 s) increased faster than the amplitudes of the other two fitted components (τ = 35–55 ms and 1.2–1.6 s, respectively), reaching a maximum after about 0.5 seconds. The amplitude of the fast and medium components started to increase after a 0.1 second lag. In other words the behavior of the slow component is what we would expect of PC, and the other two components show behavior typical of P700 (see above). The fast phase could be a recombination between $P700^+$ and the acceptor side of PSI. This interpretation is strengthened by the observation that the amplitude of this component decreases again as oxidation reaches completion after about 10 s of illumination. Under those circumstances electrons may no longer be available at the acceptor side of PSI, decreasing the likelihood of a recombination. Secondly, during the influx of electrons discussed in the previous section, the amplitude of the fast phase transiently increases in size, which is in agreement with a transient increase in the availability of electrons for charge recombination on the acceptor side of PSI. The medium phase is then the re-reduction of $P700^+$ by another electron source. The lifetime τ of the slow phase varies somewhat, depending on the circumstances but lies in the 7–14 s range.

These data indicate that the re-reduction kinetics after complete oxidation of the electron transport chain can be used to determine the relative contributions of PC and P700 to the maximum 820-nm transmission changes. Table 1 shows the contributions of PC and P700 to 820-nm changes for pea, *Camellia* and sugar beat.

Table 1 shows that the contribution of PC to the 820-nm signal was species-dependent with a 50% contribution in pea and *Camellia* and 40% in sugar beet. Comparing the relative contributions of the two P700 components, we observed that the contribution of the phase that we interpret as recombination between $P700^+$ and an electron on the acceptor side is higher in *Camellia* (30%) than in pea and sugar beet (20%).

Discussion

Nomenclature

As already observed by Harbinson and Hedley (1993), the P, S and M phases of the chl *a* fluorescence induction curve (see Papageorgiou 1975 for the nomenclature of OIDPSMT phases) are reflected in the kinetics of absorbance changes at 820 nm. As shown in Fig. 2, the I-step of the chl *a* fluorescence induction curve (see Strasser *et al.* 1995 for the nomenclature of OJIP phases) coincides quite precisely with a change in the transmission kinetics. Only a clear counter-

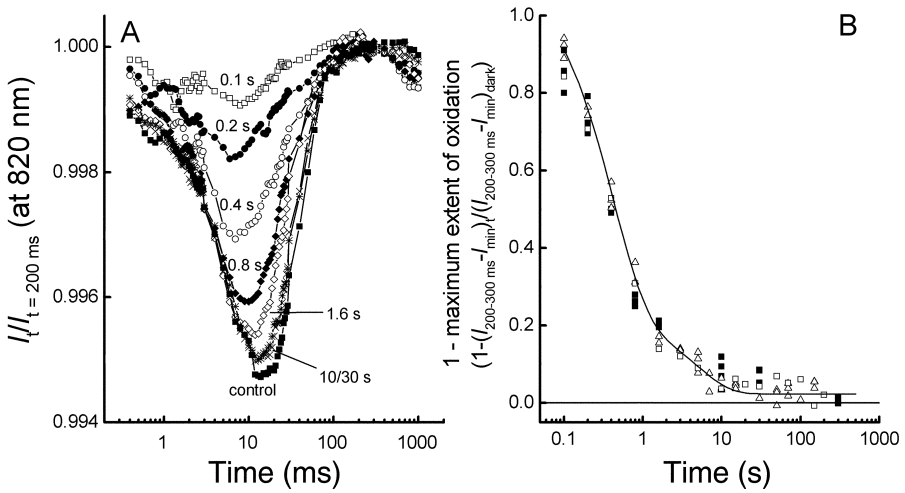

Fig. 4. Transmission induction kinetics at 820 nm as a function of time after a 1-s pulse of 1800 µmol photons m^{-2} s^{-1} in pea leaves. (*A*) Several transients measured at various intervals in the dark after the first flash. Time intervals are indicated and the induction curves were shifted to make the transmission value at t ~ 200 ms equal for all curves. Three or four curves were averaged for each measurement. (*B*) The recovery kinetics obtained in three separate experiments (see text for details). The open triangles were fitted with two exponential functions (one describing 82% of the curve with τ = 0.41 s and the other describing 18% of the curve with τ = 4.6 s); the fit-curve is also shown in part *B*.

part for the J-step seems to be missing in the transmission induction curve. To emphasize this parallelism we have chosen, in the discussion that follows, to use the fluorescence nomenclature to describe the 820-nm transmission kinetics. This means that the 'A' and 'B' of Harbinson and Woodward (1987) equal the I and P, respectively, in our figures.

Redox state of the plastoquinone pool

The dark-oxidation kinetics of a pre-reduced plastoquinone pool in leaves of higher plants is a subject that has received little attention until now. In a recent review on chlororespiration, Bennoun (2002) wrote that in higher plants the halftime of re-oxidation of the plastoquinone pool in darkness was in the 10–30 s range. Joliot and Joliot (2002) observed a halftime of re-oxidation of 20 s in spinach leaves. If the recovery kinetics of the J-level are a good measure for the re-oxidation kinetics of the plastoquinone pool in darkness, we observed a halftime of 30 s for full grown pea leaves (Strasser *et al.* 2001). In the green alga *Chlamydomonas*, chlororespiration is observed along with a re-oxidation time of the plastoquinone pool of about 3 s (e.g. Bennoun 2001); by eliminating cyt b_6/f the re-oxidation time slowed down to 31 s. It shows that without forward electron transfer, either because the electron transport chain is fully reduced or because of the absence of cyt b_6/f, the re-oxidation time of the plastoquinone pool in darkness is in the 20–30 s range. These numbers mean that the lifetime of recovery of 0.4 s for the transmission induction as observed in Fig. 4 cannot be related simply and only to the re-oxidation of the plastoquinone pool. A different approach used by Joliot and Joliot (2002) leads to the same conclusion. They observed that after a saturating light pulse the

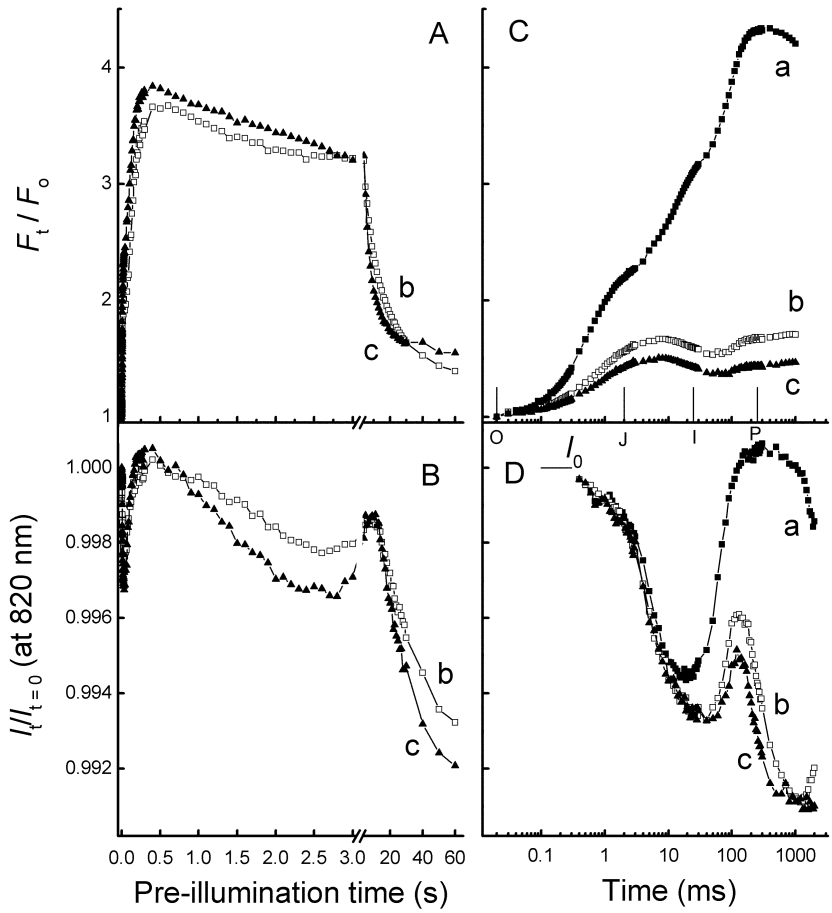

Fig. 5. Effect of a 60-s pre-illumination with 370 (b) and 740 (c) μmol photons red light m^{-2} s^{-1} [compared with no pre-illumination (a)] on the induction kinetics of the transmission at 820 nm in pea leaves. Panels *A* and *B* show the chl *a* fluorescence and 820-nm transmission changes, respectively, recorded during the pre-illumination phase of the traces b and c in panels *C* and *D*, on a linear time scale (note the change of the time scale at 3 s). (*C*) chl *a* fluorescence and (*D*) 820-nm transmission transients after induction of the Calvin–Benson cycle by the 60-s pre-illumination. The measurements in *C* and *D* were made 5 s after the 60-s pre-illumination pulse. The level I_0 indicates the transmission level just before the measurement. Three or four curves were averaged for each measurement.

complimentary area above the fluorescence induction curve recovered with biphasic kinetics. The authors assign the fast phase, with a halftime of 0.6 s, to the re-oxidation of the electron acceptors on the acceptor side of PSI. In others words, the form of the transmission induction curve during the first 200–300 ms depends on the redox state of the acceptor side of PSI and this means that the acceptor side of PSI is the rate-limiting step of this process.

Photosystem I acceptor-side limitation

Harbinson and Hedley (1993) showed that in the presence of methyl viologen and DCMU, the kinetics of the 820-nm absorbance changes were greatly simplified. The authors interpreted this result as indicating the existence of a transient, PSI acceptor-side limitation affecting the 820-nm changes beyond their point B (our P). The data in Figs 3–5 indicate that this acceptor-side limitation also plays an important role in the transmission changes observed in the time between the I and P levels of chl *a* fluorescence. Two mechanisms seem to be responsible for this acceptor-side limitation (Harbinson and Hedley 1993 and references therein). Initially, the enzyme FNR has to be activated (Carillo *et al.* 1980, 1981; Satoh 1981). Subsequently thioredoxin, taking electrons from NADPH, can activate the Calvin–Benson cycle (Buchanan 1980; Scheibe 1990). The gradual re-oxidation of PC/P700 beyond the fluorescence level P seems to indicate that FNR becomes activated shortly after the P-level is reached, and that beyond this point the limitation shifts to the Calvin–Benson cycle.

Redox state of plastocyanin, P700 and ferredoxin in a dark-adapted leaf

In a dark-adapted leaf it can be assumed that P700 is in the reduced state. The fast re-oxidation of the acceptor side of PSI ($\tau \sim 0.4$ s) interpreted from data in Fig. 4 indicates that ferredoxin will be mainly in the oxidized state. After a 1-s pulse of red (650 nm) light the whole electron transport chain is reduced including PC, P700 and ferredoxin. As shown in Fig. 1 (P-level of chl *a* fluorescence), under these circumstances the 820-nm transmission level is only slightly higher than the dark-adapted level (about 5% of the maximum reducible/oxidizable amplitude) and this increase is mainly due to the reduction of ferredoxin. The consequence of this reasoning is that PC must be in the reduced state in a dark-adapted leaf. The 5% of the amplitude mentioned above is an approximation of the maximum contribution of ferredoxin to the 820-nm transmission changes.

Reversibility of electron transport between plastocyanin and P700

If an electron donated by PC to $P700^+$ could easily return to PC^+ a clear separation between PC and P700 would become almost impossible. In the literature, two theories exist to explain electron transfer from PC to P700. The conformational change theory introduced by Bottin and Matthis (1985) assumes the electron transfer from plastocyanin to P700 is irreversible. Drepper *et al.* (1996) introduced an alternative theory that assumes that there is no conformational change but that electron transfer between PC and P700 is reversible. Olesen *et al.* (1999), studying concentration and ionic strength dependencies of a series of PC mutants, favored the conformational change theory over the reversible electron transfer, but it has to be noted that they also showed that under many conditions both theories predict the same behavior. The reason that, in both cases, the equilibrium will shift completely towards P700 is that oxidized PC will dissociate from PSI and leave its binding site. Drepper *et al.* (1996) observed a halftime of dissociation for oxidized PC of 60 μs, which is much faster than the re-reduction kinetics shown in Figs 6 and 7. In other words the ideas on electron transfer between PC and P700 support a near-complete

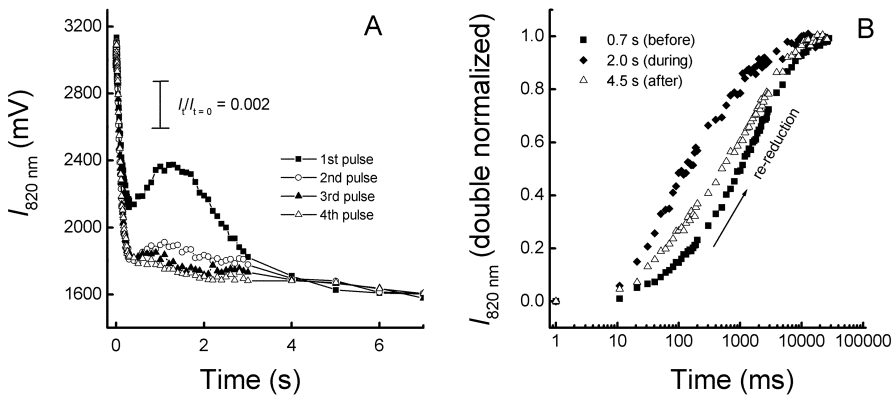

Fig. 6. Characteristics of the transient reversal of the 820-nm transmission changes during a far-red pulse (200 μmol photons m^{-2} s^{-1}). (*A*) The effect of multiple far-red pulses, spaced 100 s apart, on the 820-nm transmission transients is shown on a linear time scale. (*B*) Dark re-reduction transients initiated at three different points along the transmission transient (before, during and after the transient reversal of the 820-nm transmission) are shown.

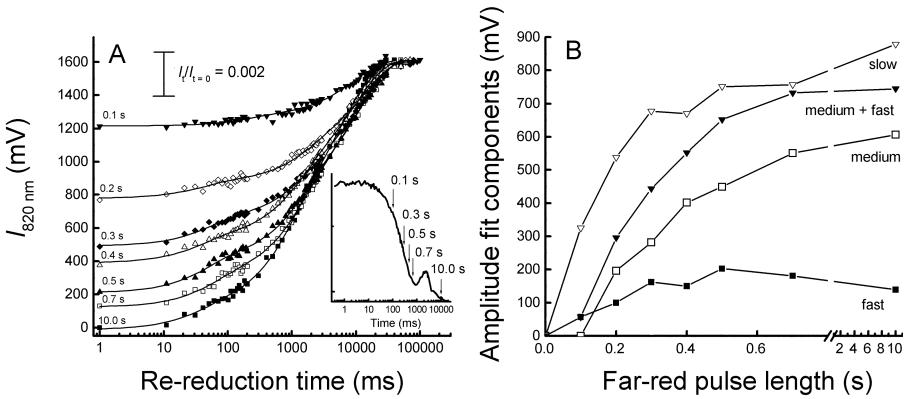

Fig. 7. (*A*) Kinetics of 820-nm transmission change in the dark after 200 μmol photons m^{-2} s^{-1} far-red pulses of different lengths. The traces were fitted with three exponential functions. (*A, inset*) a transient induced by far-red light is shown, along with an indication of where, along the transient, the far-red light was turned off for 5 of the 7 time-points shown in *A*. (*B*) The amplitudes of the three fitting components are plotted as functions of the duration of the far-red pulse. The fourth line is the sum of the fast and medium phases. The leaves were given a 10-s pre-illumination with 200 μmol photons m^{-2} s^{-1} far-red light 100 s before the start of the experiment.

separation between PC and P700 during re-reduction of the electron transport chain after a far-red pulse.

Electron sources for the re-reduction of oxidized plastocyanin and P700

During re-reduction of the electron transport chain after a far-red illumination there are two possible sources of electrons — recombination reactions (between the oxidized donors and reduced acceptors) and an influx of stromal electrons. A recombination reaction between the FeS groups $(F_AF_B)^-$ and $P700^+$ with a halftime of about 43 ms has been observed (Jordan *et al.* 1998; Ke 2001 and references therein). This is in the same time range as our fast re-reduction phase. Figure 6*B* shows that the amplitude of the fast phase remains low and has the tendency, after an initial slight increase, to decrease in size again. This behavior is consistent with a transient increase and subsequent decrease of the availability of electrons on the acceptor side of PSI during oxidation. Electrons can also come from outside of PSI and in that case there are two possibilities; $P700^+$ and PC^+ are re-reduced by separate electron pools or alternatively, $P700^+$ is reduced via PC and in that case there is a shared pool of electrons. The first option would imply that there exists an, as yet unknown, electron donor to $P700^+$ active under *in vivo* conditions in competition with PC. This would seem less likely to us. The more likely second option has as an experimental advantage that the determination of the amplitudes for P700 and PC does not depend on the donation rate of the external electron pool(s).

Contributions of plastocyanin and P700

There are several papers in which the re-reduction kinetics of $P700^+$ and of PC^+ were studied (Havaux 1996; Bukhov *et al.* 1999, 2001, 2002; Cornic *et al.* 2000). In most cases the authors have tried to manipulate the electron sources responsible for re-reduction. In the experiment depicted in Fig. 7 we did not try to manipulate the availability of electrons for re-reduction, but studied instead the oxidation of the electron transport chain by far-red light. The oxidation of the electron transport chain by far-red light was stopped at various times by turning off the far-red light and the re-reduction curves were recorded and fitted. This way, the oxidation kinetics of PC and P700 could be followed.

The assignment of the different re-reduction phases to P700 and PC is possible on the basis of our knowledge of the electron transport reactions involved. It is well known that upon absorption of a photon, P700 is oxidized within picoseconds and re-reduced by PC with halftimes of 20–200 μs (Haehnel *et al.* 1980). This means that during a far-red pulse $P700^+$ can only accumulate after oxidation of PC. Since the formation of the medium phase re-reduction phase shows a clear lag during oxidation by a far-red pulse

Table 1. Comparison of the 820-nm change kinetics in pea, *Camellia* and sugar beet leaves after a 10-s, 200 μmol photons m^{-2} s^{-1} far-red pulse

The fast:medium column gives the relative contribution of the two P700-related components (τ = 35–55 ms and 1.2–1.6 s respectively). PC = plastocyanin. The contribution values represent the mean ± s.d. of four independent experiments

		Contribution (%)	Fast:medium
Pea	P700	50.3 ± 3.0	21.0:79.0
	PC	49.7 ± 3.0	
Sugar beet	P700	60.5 ± 1.3	20.8:79.2
	PC	39.5 ± 1.3	
Camellia	P700	52.6 ± 1.6	32.8:67.2
	PC	47.4 ± 1.6	

(Fig. 7*B*) we could assign it to P700. The slow phase could be assigned to PC on the basis of two arguments. First, during the far-red pulse the slow phase was induced without a lag and second, assuming that re-reduction of $P700^+$ is mediated by PC (see above), $P700^+$ will be re-reduced first and thus, PC will have the slower re-reduction kinetics. This leaves the assignment of the fast re-reduction phase. The fast re-reduction phase has a lifetime of 35–55 ms. This is in the same time range as the 43 ms observed for the recombination reaction between $(F_AF_B)^-$ and $P700^+$ (Jordan *et al.* 1998; Ke 2001 and references therein). The limited changes in the contribution of this phase and the slight reduction observed at longer illumination times in Fig. 7*B* also point in the direction of a recombination reaction.

In agreement with the observations of other authors (Bukhov *et al.* 1999, 2001; Cornic *et al.* 2000) Fig. 6*B* shows that the re-reduction rate is faster if extra electrons are available. But the induction kinetics presented in Fig. 7 indicate that the amplitudes of the different fit components represent the electron acceptors and not the electron donors as suggested by Cornic *et al.* (2001).

The re-reduction kinetics after 10 s far-red (720 nm) light with an intensity of 200 μmol photons m^{-2} s^{-1} were analysed for leaves of pea, *Camellia* and sugar beet (Table 1). We observed a considerable variation in the relative amplitudes of PC and P700. For pea and *Camellia* both contributions were of equal size whereas in sugar beet leaves P700:PC was 60:40. Further, the two phases of P700 recovery showed differences between pea and sugar beet leaves on the one hand (~20:80) and *Camellia* leaves on the other (~30:70).

The first 8 ms

The first few milliseconds of the transmission induction curve are plotted on a linear time scale in the inset of Fig. 2*A*. The initial transmission changes can be approximated by a single exponential fit. No clear lag phase is observed and extrapolation of the curve to $t = 0$ yields a transmission value very close to the transmission level measured just before the illumination (indicated by the I_0-level). Since electrons on cytochrome f would delay the oxidation of PC and thus, would be expected to induce a lag period, this indicates that cytochrome f in dark-adapted pea leaves is mainly in the oxidized state.

Alternative electron pathways

As shown in Fig. 5, the turnover rate of the acceptor side of PSI is much lower when the Calvin–Benson cycle and the enzyme FNR are inactive. Under these circumstances ferredoxin is re-oxidized with a lifetime of ~0.4 s, whereas all the redox components of the electron transport chain can be reduced in approximately 0.2 s (at the P-level of chl *a* fluorescence). In other words, there is hardly any outflow of electrons during the period in which the electron transport chain becomes fully reduced. This means that processes like cyclic electron transfer around PSI and the Mehler reaction play no significant role during the induction of photosynthesis. This conclusion is supported by the observation that both cyclic electron transport around PSI (Cornic *et al.* 2000) and the Mehler reaction (Hormann *et al.* 1994) have to be activated, possibly by a pH gradient or low lumen pH. The data of Joliot and Joliot (2002) also seem to indicate that during the first 200–300 ms there is little cyclic electron transfer around PSI; according to their calculations cyclic electron transfer peaks around 1.5 s.

Little effect of cyclic electron transport around PSI can be expected during the first second of induction because the plastoquinone pool is very quickly reduced. Under oxidizing conditions (with far-red light), as shown in Fig. 6, there seems to be a pool of electrons with a limited capacity, the source of which is not PSII. These electrons could equate with the stromal pool of electrons described by Asada *et al.* (1992), Cornic *et al.* (2000) and Bukhov *et al.* (2001).

DCMU

Finally, the data, based on 820-nm transmission change and chl *a* fluorescence, presented in Fig. 3 confirm, in leaves, the observations made by Heber *et al.* (1988) in intact chloroplasts. These authors showed, measuring oxygen evolution, that it is necessary to inhibit a large number of the PSII reaction centers before whole-chain electron transport is affected. Comparing the traces b in Figs 3*A* and *B*, it is clear that, even when a considerable effect on the 2-ms level of the fluorescence induction curve is observed, the transmission changes are largely unaffected. The traces c show a leaf in which more than 90% of the PSII is already inhibited compared with approximately 70% of the transmission changes at 820 nm.

In summary, we conclude that it is possible to separate between the potential contributions of P700 and PC to the transmission at 820 nm by analyzing the re-reduction kinetics after a 10-s far-red pulse. We observe that PC is in the reduced state in dark-adapted leaves and is re-reduced with a τ of 7–14 s after a pulse of far-red light. The data show that *in vivo* PC makes an important contribution to the transmission changes at 820 nm.

Acknowledgments

GS and RJS acknowledge financial support from the Swiss National Foundation (3100–057046.99/1) and Govindjee acknowledges a travel grant from the University of Geneva. We thank Szilvia Zita Toth for help with the DCMU measurements and a critical reading of the manuscript.

References

Asada K, Heber U, Schreiber U (1992) Pool size of electrons that can be donated to $P700^+$, as determined in intact leaves: donation to $P700^+$ from stromal components via the intersystem chain. *Plant and Cell Physiology* **33**, 927–932.

Bennoun P (2001) Chlororespiration and the process of carotenoid biosynthesis. *Biochimica et Biophysica Acta* **1506**, 133–142.

Bennoun P (2002) The present model for chlororespiration. *Photosynthesis Research* **73**, 273–277.

Bottin H, Mathis P (1985) Interaction of plastocyanin with the photosystem I reaction center: a kinetic study by flash absorption spectroscopy. *Biochemistry* **24**, 6453–6460.

Buchanan BB (1980) Role of light in the regulation of chloroplast enzymes. *Annual Review of Plant Physiology* **31**, 341–374.

Bukhov NG, Wiese C, Neimanis S, Heber U (1999) Heat sensitivity of chloroplasts and leaves: leakage of protons from thylakoids and reversible activation of cyclic electron transport. *Photosynthesis Research* **59**, 81–93.

Bukhov N, Carpentier R, Samson G (2001) Heterogeneity of photosystem I reaction centers in barley leaves as related to the donation from stromal reductants. *Photosynthesis Research* **70**, 273–279.

Bukhov N, Egorova E, Carpentier R (2002) Electron flow to photosystem I from stromal reductants *in vivo*: the size of the pool of stromal reductants controls the rate of electron donation to both rapidly and slowly reducing photosystem I units. *Planta* **215**, 812–820.

Carillo N, Vallejos RH (1987) Ferredoxin–$NADP^+$ oxidoreductase In 'The light reactions (topics in photosynthesis, vol. 8)'. (Ed. J Barber) pp. 527–560. (Elsevier: Amsterdam)

Carrillo N, Lucero HA, Vallejos RH (1980) Effect of light on chemical modification of chloroplast ferredoxin–NADP reductase. *Plant Physiology* **65**, 495–498.

Carrillo N, Lucero HA, Vallejos RH (1981) Light modulation of chloroplast membrane-bound ferredoxin–$NADP^+$ oxidoreductase. *Journal of Biological Chemistry* **256**, 1058–1059.

Clarke JE, Johnson GN (2001) *In vivo* temperature dependence of cyclic and pseudo cyclic electron transport in barley. *Planta* **212**, 808–816.

Cornic G, Bukhov NG, Wiese C, Bligny R, Heber U (2000) Flexible coupling between light-dependent electron and vectorial proton transport in illuminated leaves of C_3 plants; role of photosystem-I-dependent proton pumping. *Planta* **210**, 468–477.

Drepper F, Hippler M, Nitschke W, Haehnel W (1996) Binding dynamics and electron transfer between plastocyanin and photosystem I. *Biochemistry* **35**, 1282–1295.

Eichelmann H, Price D, Badger M, Laisk A (2000) Photosynthetic parameters of leaves of wild type and Cyt b_6/f-deficient transgenic tobacco studied by CO_2 uptake and transmittance at 800 nm. *Plant and Cell Physiology* **41**, 432–439.

Foyer CH, Lelandais M, Harbinson J (1992) Control of the quantum efficiencies of photosystem I and II, electron flow, and enzyme activation following dark-to-light transitions in pea leaves; relationship between NADP/NADPH ratios and NADP–malate dehydrogenase activation state. *Plant Physiology* **99**, 979–986.

Haehnel W, Pröpper A, Krause H (1980) Evidence for complexed plastocyanin as the immediate electron donor of P-700. *Biochimica et Biophysica Acta* **593**, 384–399.

Harbinson J, Woodward FI (1987) The use of light-induced absorbance changes at 820 nm to monitor the oxidation state of P-700 in leaves. *Plant*, *Cell and Environment* **10**, 131–140.

Harbinson J, Hedley CL (1989) The kinetics of $P\text{-}700^+$ reduction in leaves: a novel *in situ* probe of thylakoid functioning. *Plant*, *Cell and Environment* **12**, 357–369.

Harbinson J, Foyer J (1991) Relationships between the efficiencies of photosystems I and II and stromal redox state in CO_2-free air; evidence for cyclic electron flow *in vivo*. *Plant Physiology* **97**, 41–49.

Harbinson J, Hedley CL (1993) Changes in P-700 oxidation during the early stages of the induction of photosynthesis. *Plant Physiology* **103**, 649–660.

Harbinson J, Genty B, Baker NR (1989) Relationship between the quantum efficiencies of photosystems I and II in pea leaves. *Plant Physiology* **90**, 1029–1034.

Havaux M (1996) Short-term responses of photosystem I to heat stress; induction of a PS-II-independent electron transport through PS I fed by stromal components. *Photosynthesis Research* **47**, 85–97.

Heber U, Neimanis S, Dietz K-J (1988) Fractional control of photosynthesis by the Q_B protein, the cytochrome f/b_6 complex and other components of the photosynthetic apparatus. *Planta* **173**, 267–274.

Hormann H, Neubauer C, Schreiber U (1994) An active Mehler-peroxidase reaction sequence can prevent cyclic PS I electron transport in the presence of dioxygen in intact spinach chloroplasts. *Photosynthesis Research* **41**, 429–437.

Joliot P, Joliot A (2002) Cyclic electron transfer in plant leaf. *Proceedings of the National Academy of Sciences USA* **99**, 10209–10214.

Jordan R, Nessau U, Schlodder E (1998) Charge recombination between reduced iron–sulfur clusters and P700+. In 'Photosynthesis: mechanisms and effects (vol I)'. (Ed. G Garab) pp. 663–666. (Kluwer: Dordrecht)

Katoh S (1977) Plastocyanin. In 'Encyclopedia of plant physiology (new series vol. 5)'. (Eds A Trebst and M Avron) pp. 247–252. (Springer-Verlag: Berlin)

Ke B (1973) The primary electron acceptor of photosystem I. *Biochimica et Biophysica Acta* **301**, 1–33.

Ke B (2001) Photosynthesis: photobiochemistry and photobiophysics. (Kluwer Academic Publishers: Dordrecht)

Klughammer C, Schreiber U (1991) Analysis of light-induced absorbance changes in the near-infrared spectral region; I. Characterization of various components in isolated chloroplasts. *Zeitschrift für Naturforschung* **46c**, 233–244.

Klughammer C, Schreiber U (1994) An improved method, using saturating light pulses, for the determination of photosystem I quantum yield via $P700^+$-absorbance changes at 830 nm. *Planta* **192**, 261–268.

Kramer DM, Sacksteder CA, Cruz JA (1999) How acid is the lumen? *Photosynthesis Research* **60**, 151–163.

Laisk A, Oja V, Walker D, Heber U (1992*a*) Oscillations in photosynthesis and reduction off photosystem I acceptor side in sunflower leaves; functional cytochrome b_6/f–photosystem 1 ferredoxin–NADP reductase supercomplexes. *Photosynthetica* **27**, 465–479.

Laisk A, Oja V, Heber U (1992*b*) Steady-state and induction kinetics of photosynthetic electron transport related to donor side oxidation and acceptor side reduction of photosystem I in sunflower leaves. *Photosynthetica* **27**, 449–463.

Munday JC, Govindjee (1969) Light-induced changes in the fluorescence yield of chlorophyll *a in vivo*; III. The dip and peak in the fluorescence transient of *Chlorella pyrenoidosa*. *Biophysical Journal* **9**, 1–21.

Olesen K, Ejdebäck M, Crnogorac MM, Kostic NM, Hansson Ö (1999) Electron transfer to photosystem I from spinach plastocyanin mutated in the small acidic patch: ionic strength dependence of kinetics and comparison of mechanistic models. *Biochemistry* **38**, 16695–16705.

Ott T, Clarke J, Birks K, Johnson G (1999) Regulation of the photosynthetic electron transport chain. *Planta* **209**, 250–258.

Papageorgiou G (1975) Chlorophyll fluorescence: an intrinsic probe of photosynthesis. In 'Bioenergetics of photosynthesis'. (Ed. Govindjee) pp. 319–371. (Academic Press: New York, NY)

Samson G, Prasil O, Yaacoubd B (1999) Photochemical and thermal phases of chlorophyll *a* fluorescence. *Photosynthetica* **37**, 163–182.

Satoh K (1981) Fluorescence induction and activity of ferredoxin–$NADP^+$ reductase in *Bryopsis* chloroplasts. *Biochimica et Biophysica Acta* **638**, 327–333.

Scheibe R (1990) Light/dark modulation: regulation of chloroplast metabolism in a new light. *Botanica Acta* **103**, 327–334.

Schreiber U, Klughammer C, Neubauer C (1988) Measuring P700 absorbance changes around 830 nm with a new type of pulse modulation system. *Zeitschrift für Naturforschung* **43c**, 686–698.

Strasser RJ, Srivastava A and Govindjee (1995) Polyphasic chlorophyll a fluorescence transient in plants and cyanobacteria. *Photochemistry and Photobiology* **61**, 32–42.

Strasser RJ, Schansker G, Srivastava A, Govindjee (2001) [CD–ROM computer file] Simultaneous measurement of photosystem I and photosystem II probed by modulated transmission at 820 nm and by chlorophyll *a* fluorescence in the sub ms to second time range. In 'Proceedings of the 12th international congress on photosynthesis' Brisbane. S14–003. (CSIRO Publishing: Melbourne, Vic.)

van Voorthuysen T (1997) The electrical potential as a gauge of photosynthetic performance in plant chloroplasts; a patch-clamp study. (Wageningen Agricultural University: Wageningen)

Weis E, Lechtenberg D (1989) Fluorescence analysis during steady state photosynthesis. *Philosophical Transactions of the Royal Society of London, series B* **323**, 253–268.

Witt HT (1971) Coupling of quanta, electrons, fields, ions and phosphorylation in the functional membrane of photosynthesis; results by pulse spectroscopic methods. *Quarterly Review of Biophysics* **4**, 365–477.

Manuscript received 11 February 2003, accepted 2 June 2003